Star Formation Newsletter
No. 334 29-35

高橋実道（NAOJ）

29. **The SOFIA Massive (SOMA) Star Formation Survey. III. From Intermediate- to High-Mass Protostars**

Mengyao Liu[1], Jonathan C. Tan[2,1], James M. De Buizer[3], Yichen Zhang[4], Emily Moser[5], Maria T. Beltrán[6], Jan E. Staff[7], Kei E. I. Tanaka[8], Barbara Whitney[9], Viviana Rosero[10], Yao-Lun Yang[1] and Rubén Fedriani[2]

30. **ALMA observations and modeling of the rotating outflow in Orion Source I**

J. A. López-Vázquez[1], Luis A. Zapata[1], Susana Lizano[1] and Jorge Cantó[2]

31. **Failed and delayed protostellar outflows with high mass accretion rates**

Masahiro N. Machida[1] and Takashi Hosokawa[2]

32. **Exploring the nature of compact radio sources associated to UCHII regions**

J.M. Masqué[1], L.F. Rodríguez[2,3], S.A. Dzib[4], S.N. Medina[4], L. Loinard[2], M.A. Trinidad[1], S.E. Kurtz[2] and C. A Rodríguez-Rico[1]

33. **ALMA observations of envelopes around first hydrostatic core candidates**

María José Maureira[1,2], Héctor G. Arce[1], Michael M. Dunham[3,4], Diego Mardones[5,2], Andrés E. Guzmán[6], Jaime E. Pineda[2] and Tyler L. Bourke[7,3]

34. **Carbon depletion observed inside T Tauri inner rims: Formation of icy, kilometer size planetesimals by 1 Myr**

M. K. McClure[1]

35. **Measuring the atomic composition of planetary building blocks**

Melissa McClure[1], Carsten Dominik[2] and Mihkel Kama[3]

29. **The SOFIA Massive (SOMA) Star Formation Survey. III. From Intermediate- to High-Mass Protostars**

Mengyao Liu[1], Jonathan C. Tan[2,1], James M. De Buizer[3], Yichen Zhang[4], Emily Moser[5], Maria T. Beltrán[6], Jan E. Staff[7], Kei E. I. Tanaka[8], Barbara Whitney[9], Viviana Rosero[10], Yao-Lun Yang[1] and Rubén Fedriani[2]

We present $\sim 10-40\,\mu$m *SOFIA*-FORCAST images of 14 intermediate-mass protostar candidates as part of the *SOFIA* Massive (SOMA) Star Formation Survey. We build spectral energy distributions (SEDs), also utilizing archival *Spitzer*, *Herschel* and *IRAS* data. We then fit the SEDs with radiative transfer (RT) models of Zhang & Tan (2018), based on Turbulent Core Accretion theory, to estimate key protostellar properties. With the addition of these intermediate-mass sources, SOMA protostars span luminosities from $\sim 10^2-10^6\,L_\odot$, current protostellar masses from $\sim 0.5-30\,M_\odot$ and ambient clump mass surface densities, $\Sigma_{\rm cl}$ from $0.1-3\,{\rm g\,cm^{-2}}$. A wide range of evolutionary states of the individual protostars and of the protocluster environments are also probed. We have also considered about 50 protostars identified in Infrared Dark Clouds and expected to be at the earliest stages of their evolution. With this global sample, most of the evolutionary stages of high- and intermediate-mass protostars are probed. From the best fitting models, there is no evidence of a threshold value of protocluster clump mass surface density being needed to form protostars up to $\sim 25\,M_\odot$. However, to form more massive protostars, there is tentative evidence that $\Sigma_{\rm cl}$ needs to be $\gtrsim 1\,{\rm g\,cm^{-2}}$. We discuss how this is consistent with expectations from core accretion models that include internal feedback from the forming massive star.

SOFIA-FORCASTで14のintermediate-mass protostar の撮像

Spitzer, Herschel, IRASの結果と合わせたSEDを輻射輸送計算と比較。

他の結果と合わせて64個のprotostar について調べる。

Luminosity 10^2-10^6Lsun, Mass 0.5-30Msun, clump mass surface density 0.1-3 g/cm^2

clump mass surface density について、<25Msun には傾向なし。

>25Msun には>1g/cm^2が必要。

30. **ALMA observations and modeling of the rotating outflow in Orion Source I**

J. A. López-Vázquez[1], Luis A. Zapata[1], Susana Lizano[1] and Jorge Cantó[2]

We present ^{29}SiO(J=8–7) ν=0, SiS (J=19–18) ν=0, and ^{28}SiO (J=8–7) ν=1 molecular line archive observations made with the Atacama Large Millimeter/Submillimeter Array (ALMA) of the molecular outflow associated with Orion Source I. The observations show velocity asymmetries about the flow axis which are interpreted as outflow rotation. We find that the rotation velocity (∼4–8 km s^{-1}) decreases with the vertical distance to the disk. In contrast, the cylindrical radius (∼100–300 au), the expansion velocity (∼2–15 km s^{-1}), and the axial velocity v_z (∼-1–10 km s^{-1}) increase with the vertical distance. The mass estimated of the molecular outflow $M_{outflow}$ ∼0.66–1.3 $M_\odot$. Given a kinematic time ∼130 yr, this implies a mass loss rate $\dot{M}_{outflow} \sim 5.1 - 10 \times 10^{-3}$ $M_\odot$ yr^{-1}. This massive outflow sets important contraints on disk wind models. We compare the observations with a model of a shell produced by the interaction between an anisotropic stellar wind and an Ulrich accretion flow that corresponds to a rotating molecular envelope in collapse. We find that the model cylindrical radii are consistent with the ^{29}SiO(J=8–7) ν=0 data. The expansion velocities and the axial velocities of the model are similar the observed values, except close to the disk ($z \sim \pm 150$ au) for the expansion velocity. Nevertheless, the rotation velocities of the model are a factor ∼3–10 lower than the observed values. We conclude that the Ulrich flow alone cannot explain the rotation observed and other possibilities should be explored, like the inclusion of the angular momentum of a disk wind.

ALMAのアーカイブデータを使ってOrion Source I のmolecular outflowについて解析

outflowの回転が見えている

outflow mass ~ 0.66-1.2Msun, -> mass loss rate ~ 5.1-10 x10^{-3} Msun/yr. (kinematic time~130yr)

観測されたoutflow のshell が、stellar wind と回転しながら落下するenvelope とのinteraction だとすると、回転速度以外がモデルと一致。

Molecular Outflow

二つの説

1：純粋な円盤起源

2：stellar wind とinfalling envelope の相互作用で形成

outflowの質量が大きすぎる場合、2が有力

例：DG Tau B

mass loss rate ~ (1.7-2.9) x10^{-7} Msun/yr,

disk mass ~ 0.068 Msun

-> disk lifetime ~ (2-4)x10^{5} yr

< age of DG Tau B

本論文の対象：Orion Source I

距離 418pc, M* > 8Msun, L*~10^{4} Lsun

outflow velocity ~ 18 km/s

このoutflowも質量が大きく、2が有力

2についてのmodelを使って観測をfitしてみる。

観測

ALMA Band7

^{28}SiO, ^{29}SiO, SiSのlineのアーカイブデータを使用

	rms noise	Beam size
^{28}SiO, SiS	10 mJy/Beam	0.19” x 0.14”
^{29}SiO	20 mJy/Beam	0.30” x 0.24”

^{29}SiO　　SiS　　^{28}SiO

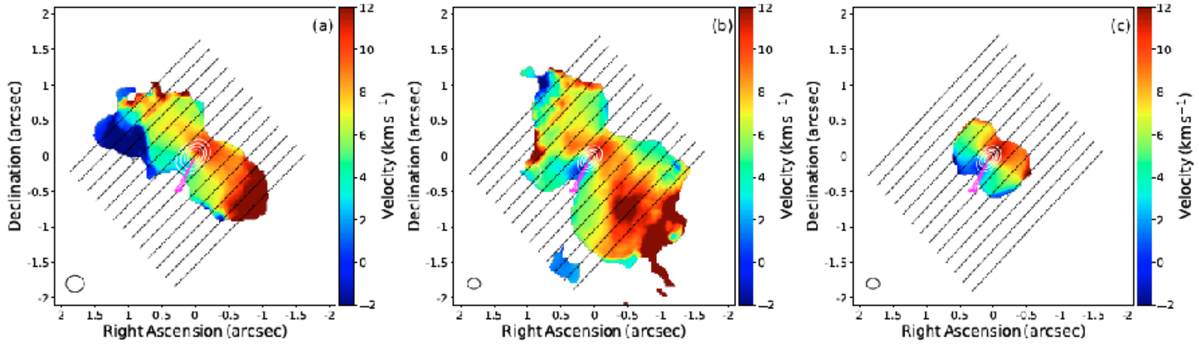

^{29}SiO, SiS で480 au のアウトフロー

回転も見える

アウトフローの各高さでのPV図

例：^{29}SiO

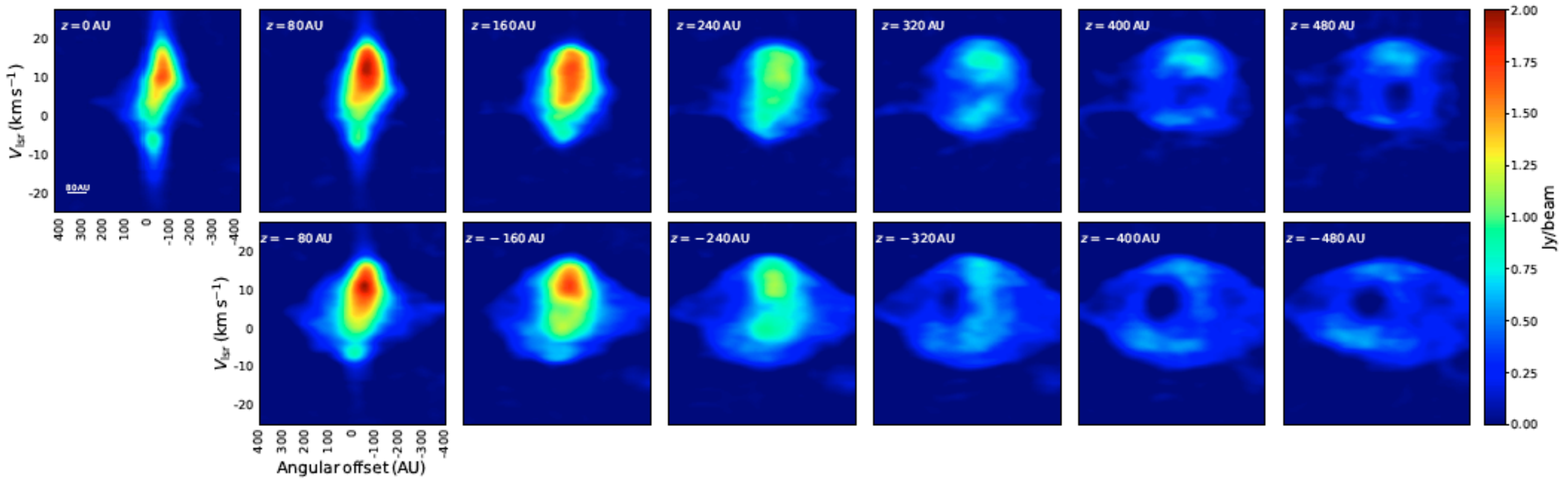

上空でexpanding shell
速度の非対称性 → 回転

アウトフローの質量, Disk life time

^{28}SiOは光学的に厚いとする→ 温度
^{29}SiOから質量を得る

^{28}SiO/H_2 = 1.2-2.4x10^{-7}とすると

Moutflow > 0.66-1.3 Msun

outflow size =480 au,
velocity v~ 18 km/s
-> kinematic time ~130 yr
mass loss late 5.1-10x10^{-3} Msun/yr

disk mass < 5 Msun
-> disk life time ~ 1000 yr
短すぎる。stellar wind とenvelope が起源か？

モデルとの比較

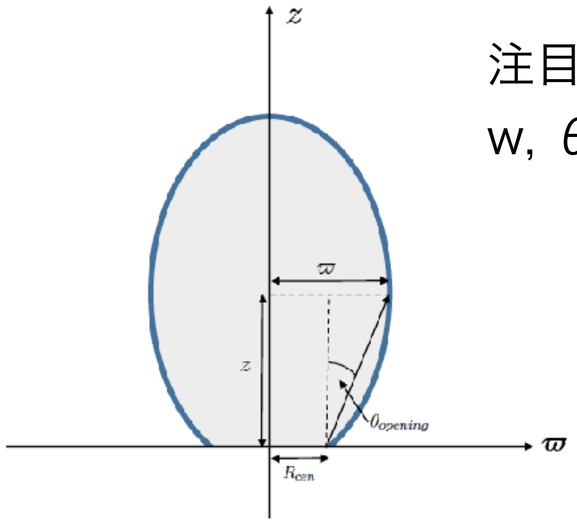

注目する物理量は
w, θ , v_z, v_exp, v_rotの五つ

モデルパラメータ
（Lopez-Vazquez+2019）

$$\alpha = \frac{\dot{\mathrm{M}}_w}{\dot{\mathrm{M}}_a}, \qquad \beta = \frac{\dot{\mathrm{M}}_w v_w}{\dot{\mathrm{M}}_a v_0} = \alpha \frac{v_w}{v_0},$$

Stellar wind のdensity prolfile

$$\rho_w = \frac{\dot{\mathrm{M}}_w}{4\pi r^2 v_w} f(\theta), \qquad f(\theta) = \frac{A + B\cos^{2n}\theta}{A + B/(2n+1)}.$$

Best fit model

α=0.1, β=4, A=1, B=35, n=5

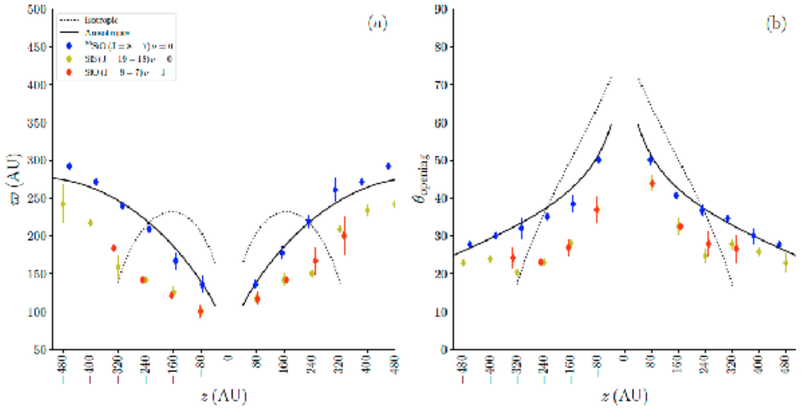

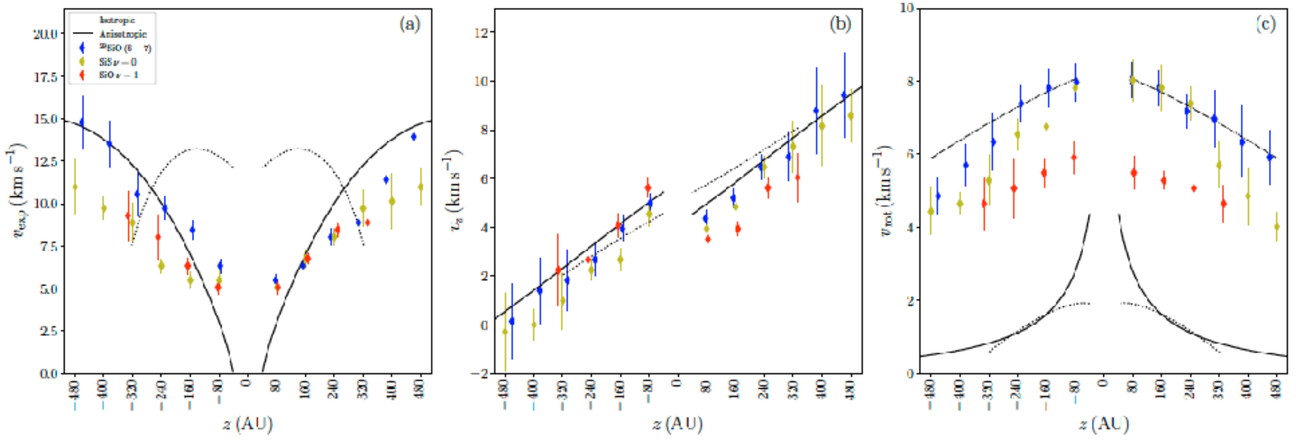

回転速度以外はよく合うが、回転速度が3-10倍ずれる。
円盤からの角運動量の供給が必要か。

31. **Failed and delayed protostellar outflows with high mass accretion rates**

Masahiro N. Machida[1] and Takashi Hosokawa[2]

The evolution of protostellar outflows is investigated under different mass accretion rates in the range $\sim 10^{-5}$–$10^{-2}\,\mathrm{M_\odot\,yr^{-1}}$ with three-dimensional magnetohydrodynamic simulations. A powerful outflow always appears in strongly magnetized clouds with $B_0 > B_{0,\mathrm{cr}} = 10^{-4}(M_{\mathrm{cl}}/100\,\mathrm{M_\odot})\,\mathrm{G}$, where M_{cl} is the cloud mass. When a cloud has a weaker magnetic field, the outflow does not evolve promptly with a high mass accretion rate. In some cases with moderate magnetic fields B_0 slightly smaller than $B_{0,\mathrm{cr}}$, the outflow growth is suppressed or delayed until the infalling envelope dissipates and the ram pressure around the protostellar system is significantly reduced. In such an environment, the outflow begins to grow and reaches a large distance only during the late accretion phase. On the other hand, the protostellar outflow fails to evolve and is finally collapsed by the strong ram pressure when a massive ($> 100\mathrm{M_\odot}$) initial cloud is weakly magnetized with $B_0 < 100\,\mu\mathrm{G}$. The failed outflow creates a toroidal structure that is supported by magnetic pressure and encloses the protostar and disk system. Our results indicate that high-mass stars form only in strongly magnetized clouds, if all high-mass protostars possess a clear outflow. If we would observe either very weak or no outflow around evolved protostars, it means that strong magnetic fields are not necessarily required for high-mass star formation. In any case, we can constrain the high-mass star formation process from observations of outflows.

質量降着率が大きい場合(10^{-5}-10^{-2} Msun/yr)のoutflowについての3DMHDシミュレーション

outflowは磁場が強い場合に駆動される。 $B_0 \gtrsim B_{0,\mathrm{cr}} = 10^{-4}(M_{\mathrm{cl}}/100\,\mathrm{M_\odot})\,\mathrm{G},$

Marginal な磁場では、原始星形成後＞1000 yr からのみoutflowが見られる場合がある。

星形成に常にoutflowが付随するなら、大質量星は常に強磁場の環境で形成される。

outflowが付随しない星形成が観測されれば、大質量星形成に強磁場は必要ない。

モデルパラメータと結果のまとめ

Model	f	μ_0	B_0 [G]	Ω_0 [s^{-1}]	α_0	β_0	γ_0	M_{cl} [$M_\odot$]	Outflow	frag.
AM2	1.4	2	1.5×10^{-5}				0.19		Successful	N
AM3	1.4	3	1.0×10^{-5}				0.083		Successful	N
AM5	1.4	5	6.2×10^{-6}	3.2×10^{-14}	0.5	0.02	0.030	11	Delayed	N
AM10	1.4	10	3.1×10^{-6}				7.5×10^{-3}		Delayed	N
AM20	1.4	20	1.6×10^{-6}				1.9×10^{-3}		Delayed	N
BM2	3.4	2	3.8×10^{-5}				0.19		Successful	N
BM3	3.4	3	2.5×10^{-5}				0.083		Successful	N
BM5	3.4	5	1.5×10^{-5}	5.0×10^{-14}	0.2	0.02	0.030	28	Delayed	N
BM10	3.4	10	7.5×10^{-6}				7.5×10^{-3}		Failed	N
BM20	3.4	20	3.7×10^{-6}				1.9×10^{-3}		Failed	N
CM2	8.4	2	9.2×10^{-5}				0.19		Successful	N
CM3	8.4	3	6.2×10^{-5}				0.083		Successful	N
CM5	8.4	5	3.7×10^{-5}	7.9×10^{-14}	0.08	0.02	0.030	68	Failed	N
CM10	8.4	10	1.9×10^{-5}				7.5×10^{-3}		Failed	N
CM20	8.4	20	6.2×10^{-6}				1.9×10^{-3}		Failed	N
DM2	16.8	2	1.9×10^{-4}				0.19		Successful	N
DM3	16.8	3	1.2×10^{-4}				0.083		Successful	N
DM5	16.8	5	7.4×10^{-5}	1.1×10^{-13}	0.04	0.02	0.030	132	Failed	N
DM10	16.8	10	3.7×10^{-5}				7.5×10^{-3}		Failed	Y (2)
DM20	16.8	20	1.8×10^{-5}				1.9×10^{-3}		Failed	N
EM2	33.6	2	3.7×10^{-4}				0.19		Successful	N
EM3	33.6	3	2.4×10^{-4}				0.083		Successful	N
EM5	33.6	5	1.5×10^{-4}	1.5×10^{-13}	0.02	0.02	0.030	272	Delayed	Y (4)
EM10	33.6	10	7.4×10^{-5}				7.5×10^{-3}		Failed	Y (4)
EM20	33.6	20	3.7×10^{-5}				1.9×10^{-3}		Failed	Y (4)
FM2	67.2	2	7.4×10^{-4}				0.19		Successful	Y (2)
FM3	67.2	3	5.0×10^{-4}				0.083		Delayed	Y (6)
FM5	67.2	5	3.0×10^{-4}	2.2×10^{-13}	0.01	0.02	0.030	545	Delayed	Y (6)
FM10	67.2	10	1.5×10^{-4}				7.5×10^{-3}		Delayed	Y (4)
FM20	67.2	20	7.4×10^{-5}				1.9×10^{-3}		Failed	Y (8)

A -> Fの順に大質量になる。

末尾の数字がmass-to-flax ratio, ~5 以下でoutflowが駆動

例：DM 2, 5, 10

outflow　成功　失敗　失敗

t

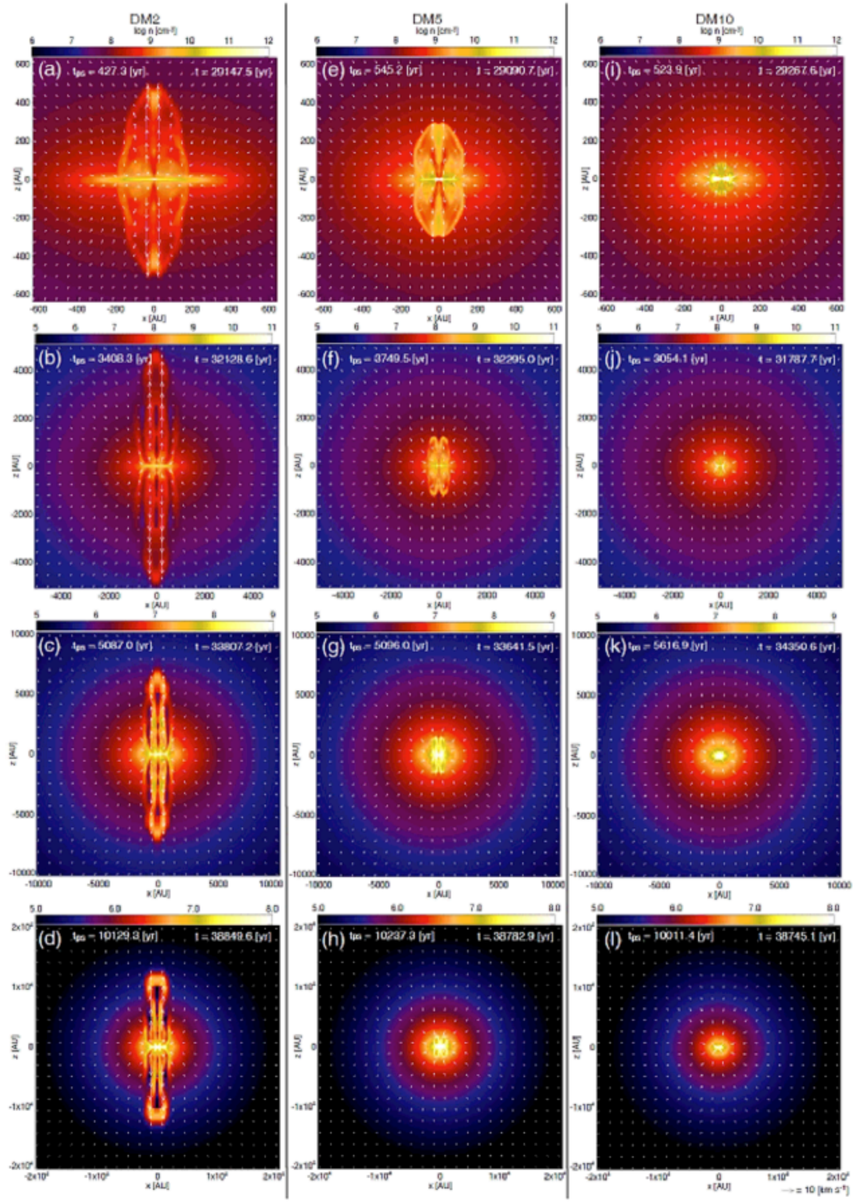

Delayed outflow の例：FM 10

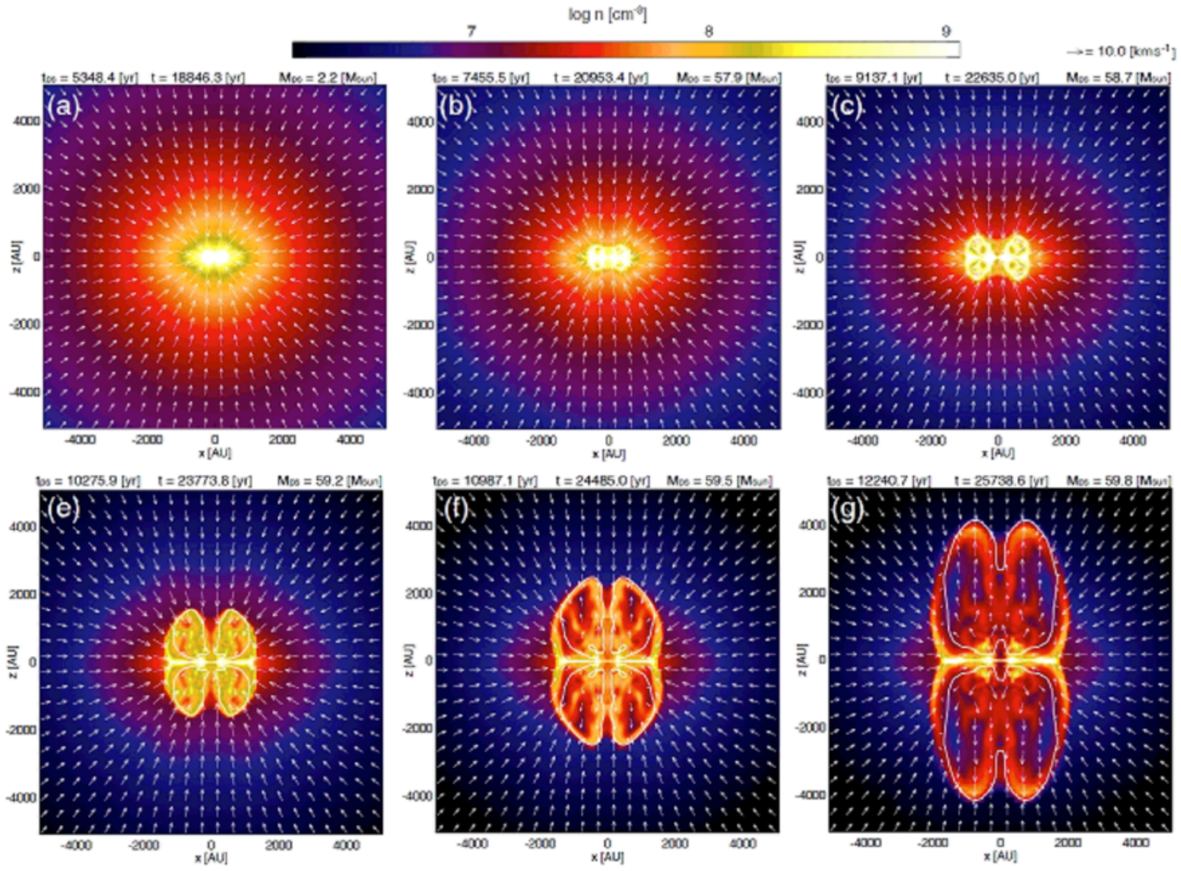

Outflow size

実線：Successful, 点線：Delayed, 破線：Failed

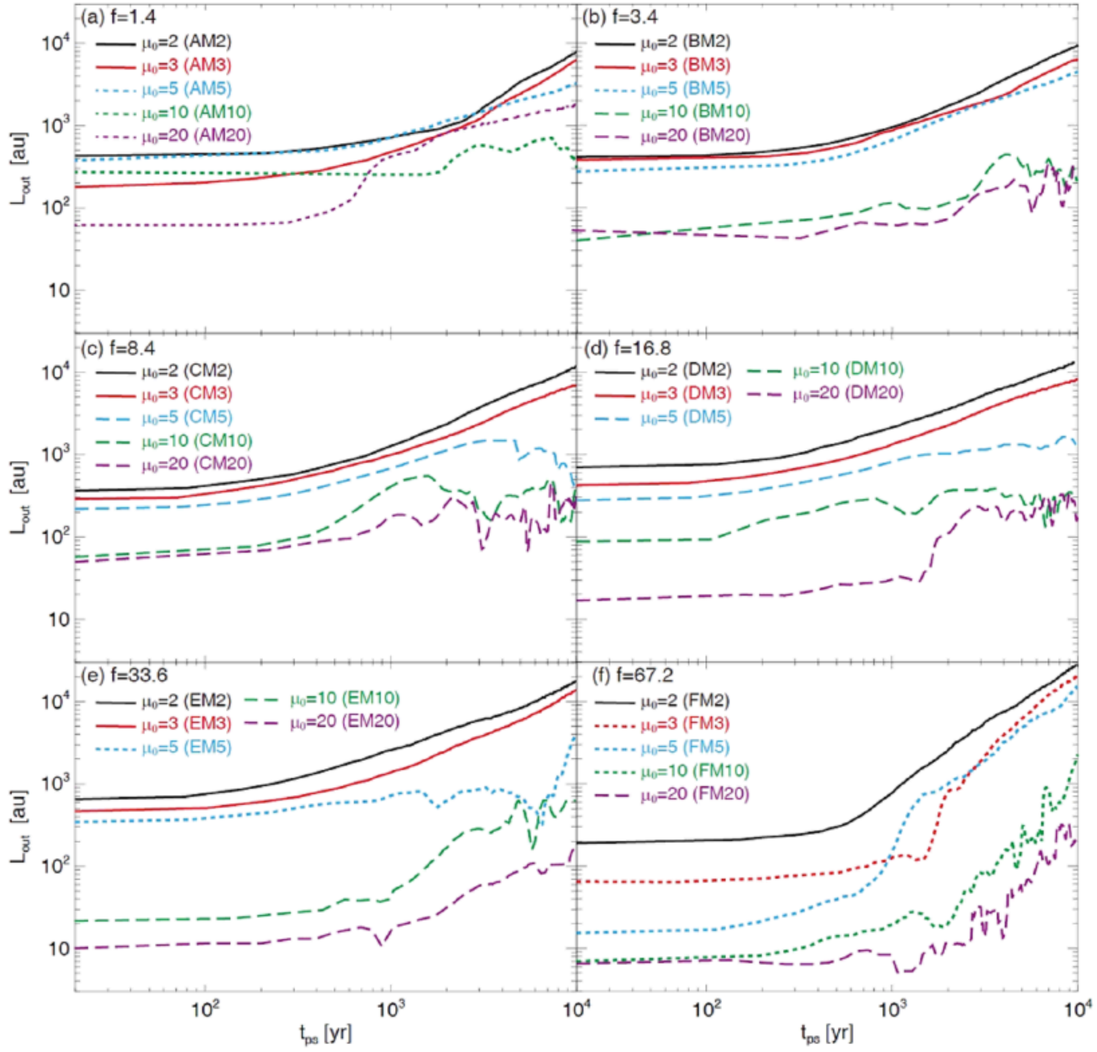

32. Exploring the nature of compact radio sources associated to UCHII regions

J.M. Masqué[1], L.F. Rodríguez[2,3], S.A. Dzib[4], S.N. Medina[4], L. Loinard[2], M.A. Trinidad[1], S.E. Kurtz[2] and C. A Rodríguez-Rico[1]

We present Very Large Array 7 mm continuum observations of four Ultra-Compact (UC)HII regions, observed previously at 1.3 cm, in order to investigate the nature of the compact radio sources associated with these regions. We detected a total of seven compact radio sources, four of them with thermal emission, and two compact radio sources have clear non-thermal emission. The thermal emission is consistent with the presence of an ionized envelope, either static (i.e., trapped in the gravitational radius of an associated massive star) or flowing away (i.e., a photo-evaporative flow). On the other hand, the nature of the non-thermal sources remains unclear and several possibilities are proposed. The possibility that most of these compact radio sources are photo-evaporating objects and the remaining ones more-evolved objects is consistent with previous studies on UCHII regions.

VLAによる4つのUltra-Compact (UC) HII region の観測。7mm continuum
compact radio sources が付随　7個をdetect
4個がthermal emission, 3個がnon-thermal emissionを持つ

thermal emission -> ionized envelope (i.e. photo-evaporative flow)
non-thermal emission -> more-evolved object?

33. **ALMA observations of envelopes around first hydrostatic core candidates**

María José Maureira[1,2], Héctor G. Arce[1], Michael M. Dunham[3,4], Diego Mardones[5,2], Andrés E. Guzmán[6], Jaime E. Pineda[2] and Tyler L. Bourke[7,3]

We present ALMA 3 mm molecular line and continuum observations with a resolution of 3.5" towards five first hydrostatic core (FHSC) candidates (L1451-mm, Per-bolo 58, Per-bolo 45, L1448-IRS2E and Cha-MMS1). Our goal is to characterize their envelopes and identify the most promising sources that could be bona fide FHSCs. We identify two candidates which are consistent with an extremely young evolutionary state (L1451-mm and Cha-MMS1), with L1451-mm being the most promising FHSC candidate. Although our envelope observations cannot rule out Cha-MMS1 as a FHSC yet, the properties of its CO outflow and SED published in recent studies are in better agreement with the predictions for a young protostar. For the remaining three sources, our observations favor a prestellar nature for Per-bolo 45 and rule out the rest as FHSC candidates. Per-bolo 58 is fully consistent with being a Class 0, while L1448 IRS2E shows no emission of high-density tracers (NH2D and N2H+) at the location of the previously identified compact continuum source, which is also undetected in our observations. Thus we argue that there is no embedded source at the presumptive location of the FHSC candidate L1448 IRS2E. We propose instead, that what was thought to be emission from the presumed L1448 IRS2E outflow corresponds to outflow emission from a nearby Class 0 system, deflected by the dense ambient material. We compare the properties of the FHSC candidates studied in this work and the literature, which shows that L1451-mm appears as possibly the youngest source with a confirmed outflow.

ALMA 3mm の観測で、５つのfirst hydrostatic core (FHSC)のcandidate のenvelope を観測。
（L1451-mm, Per-bolo 58, Per-bolo 45, L1448-IRS2E, Cha-MMS1）

もっともFHCSらしい天体はどれか？

L1451-mm がoutflowが見える中で最も若い天体。

Cha-MMS1はCO outflow やSEDからprotostar と考えられる。

Per-bolo45は prestellar, Per-bolo 58はClass 0

L1448IRS2E high-density tracer が受かっていない

First hydrostatic core (FHSC)

星形成理論で、星形成の最初期に形成されると
考えられている天体。
低質量(<0.1Msun)で短寿命(~10^4 yr)
短寿命のため、観測が困難。
これまでいくつかの候補天体が見つかっている。

FHSC候補天体
<70um が非常に弱いor 見えない
compact continuum source, small outflowが付随

Molecular line の重要性
温度が高い兆候（>20-30K）は見えないはず

infall velocity は中心天体が低質量(<0.1Msun)
と整合的となるはず。

本論文では、ALMAの3mmのline と連続波で
5つのFHSC候補天体を3.5”-4”の分解能で観測

観測

ALMA Cycle 1

terget

Source	$M_{core}(M_\odot)$	$L_{int}(L_\odot)$	24μm ? [a]	CO_{out} lobe length[b]	CO_{out} velocity[b]	Distance	Ref.
L1448 IRS2E	2.3	< 0.035	No	1114 au	25 km s^{-1}	290 pc	1
Per-bolo 45	2.1	< 0.021	No	...	...	290 pc	2
Per-bolo 58	0.7	0.020	Yes	7192 au	3 km s^{-1}	290 pc	3
L1451-mm	0.3	< 0.021	No	638 au	1 km s^{-1}	290 pc	4
Cha-MMS1	0.6	0.021	Yes	2470 au	2-12 km s^{-1}	190 pc	5

lineや分解能など

Source	Map	Rest Frequency (GHz)	Synthesized Beam	PA	RMS (mJy beam^{-1})
L1448-IRS2E	$NH_2D(1_{1,1}\text{-}1_{0,1})$	85.926	5.4"×2.8"	-32°	24
(12m + 7m)	N_2H^+(1-0)	93.173	4.2"×3.0"	17°	24
	HCN(1-0)	88.632	5.3"×2.7"	33°	34
Phase center (J2000)	$H^{13}CO^+$(1-0)	86.754	5.4"×2.8"	-34°	26
03h 25m 25.66s	HCO^+(1-0)	89.189	5.4"×2.8"	-33°	29
+30d 44m 56.70s	$CH_3OH(2_{0,2}\text{-}1_{0,1})$	96.741	4.1"×2.9"	19°	24
	$CH_3OH(3_{1,3}\ 4_{0,4})$	107.014	3.6"×2.6"	16°	25
	3mm continuum	103.55	3.5"×2.5"	16°	0.15
Per-bolo 45	$NH_2D(1_{1,1}\text{-}1_{0,1})$	85.926	5.4"×3.8"	-32°	34
(12m + 7m)	N_2H^+ (1-0)	93.173	4.2"×3.0"	14°	21
	HCN(1-0)	88.632	5.8"×2.7"	33°	34
Phase center (J2000)	$H^{13}CO^+$(1-0)	86.754	5.4"×2.8"	34°	26
03h 29m 07.70s	HCO^+(1-0)	89.189	5.5"×2.8"	-34°	29
+31d 17m 16.80s	$CH_3OH(2_{0,2}\text{-}1_{0,1})$	96.741	4.0"×2.8"	16°	22
	$CH_3OH(3_{1,3}\ 4_{0,4})$	107.014	3.6"×2.6"	15°	24
	3mm continuum	103.55	3.5"×2.5"	13°	0.15
Per-bolo 58	$NH_2D(1_{1,1}\text{-}1_{0,1})$	85.926	5.5"×2.8"	32°	38
(12m + 7m)	N_2H^+(1-0)	93.173	4.2"×3.0"	17°	21
	HCN(1-0)	88.632	5.4"×2.7"	-34°	34
Phase center (J2000)	$H^{13}CO^+$(1-0)	86.754	5.5"×2.8"	34°	26
03h 29m 25.46s	HCO^+(1-0)	89.189	5.5"×2.8"	33°	29
+31d 28m 15.00s	$CH_3OH(2_{0,2}\text{-}1_{0,1})$	96.741	4.1"×2.8"	17°	22
	$CH_3OH(3_{1,3}\text{-}4_{0,4})$	107.014	3.6"×2.6"	15°	25
	3mm continuum	103.55	3.5"×2.4"	14°	0.15
L1451-mm	$NH_2D(1_{1,1}\text{-}1_{0,1})$	85.926	5.4"×2.8"	-33°	34
(12m + 7m)	N_2H^+(1-0)	93.173	4.1"×3.0"	16°	20
	HCN(1-0)	88.632	5.3"×2.7"	-34°	34
Phase center (J2000)	$H^{13}CO^+$(1-0)	86.754	5.4"×2.8"	-34°	26
03h 25m 10.21s	HCO^+(1-0)	89.189	5.4"×2.8"	-34°	29
30d 23m 55.30s	$CH_3OH(2_{0,2}\ 1_{0,1})$	96.741	4.0"×2.8"	17°	21
	$CH_3OH(3_{1,3}\text{-}4_{0,4})$	107.014	3.6"×2.6"	14°	25
	3mm continuum	103.55	3.5"×2.5"	14°	0.14
Cha-MMS1	$NH_2D(1_{1,1}\text{-}1_{0,1})$	85.926	3.1"×1.8"	11°	14
(12m + 7m + TP)	N_2H^+ (1-0)	93.173	2.8"×1.8"	11°	20
	HCN(1-0)	88.632	3.0"×1.8"	11°	13
Phase center (J2000)	$H^{13}CO^+$(1-0)	86.754	3.1"×1.8"	12°	15
11h 06m 31.23s	HCO^+(1-0)	89.189	3.0"×1.8"	12°	14
-77d 23m 33.57s	$CH_3OH(2_{0,2}\ 1_{0,1})$	96.741	2.7"×1.8"	11°	22
	$CH_3OH(3_{1,3}\text{-}4_{0,4})$	107.014	2.5"×1.6"	-10°	27
	3mm cont (12m+7m only)	103.55	2.5"×1.6"	-7°	0.13

観測結果

例：L1451-mm

連続波

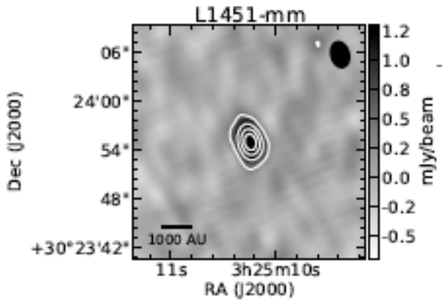

mass 0.28Msun

Line: moment 0, 1, 2

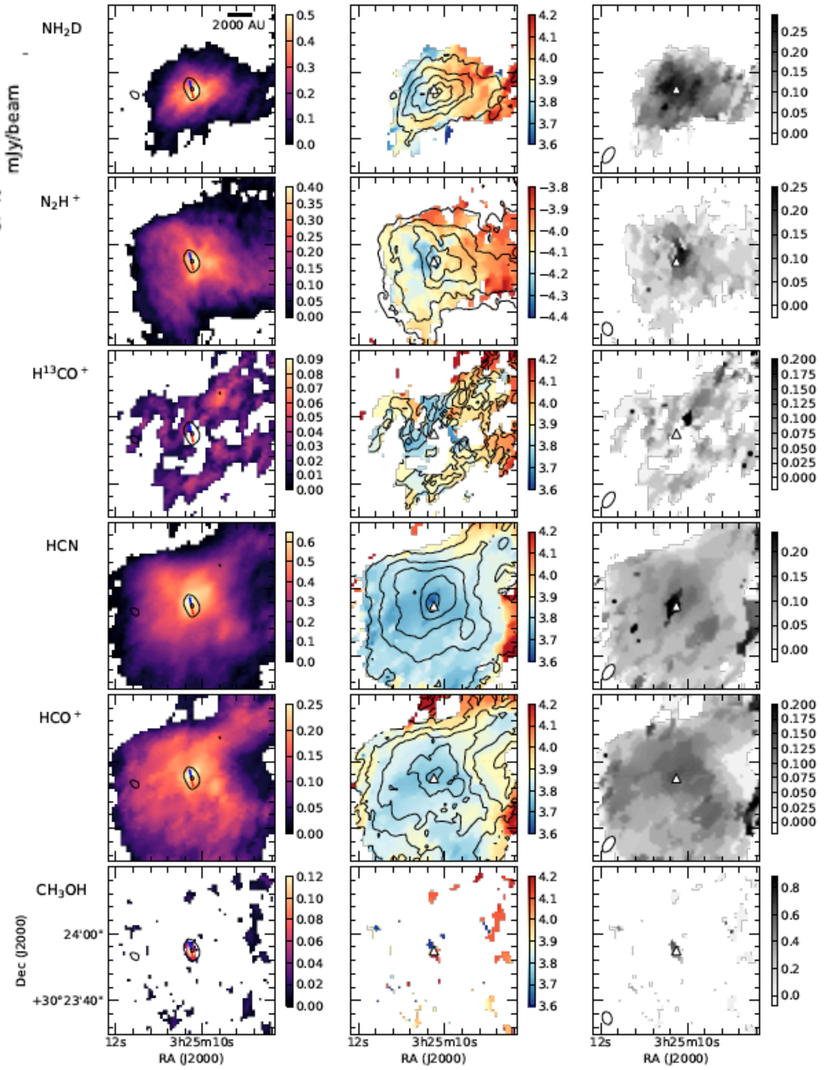

H13CO+が見えない

炭素系の分子がfrozen outしている

（prestellar coreでよくある）

非常に若い天体であることを示唆

（HCO+, HCNは量が多いために見える）

NH2D, N2H+ のPV図のmodel fitから、

central mass 0.04 Msun, 0.08 Msun

FHSCや若いprotosterと整合的

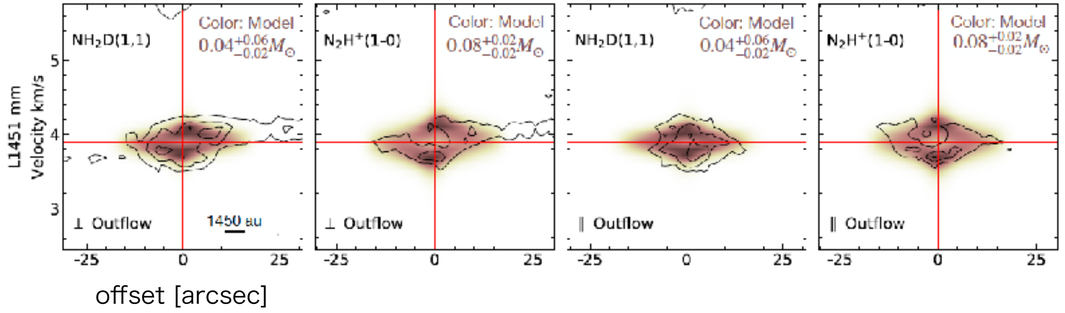

HCN, CH3OH で大きな速度分散

→コンパクトな outflow (<1000au)

以上の結果から、L1451-mmは最も若い

protostellar source の一つ→FHSC candidate

34. Carbon depletion observed inside T Tauri inner rims: Formation of icy, kilometer size planetesimals by 1 Myr

M. K. McClure[1]

Context: The carbon content of protoplanetary disks is an important parameter to characterize planets formed at different disk radii. There is some evidence from far-infrared and submillimeter observations that gas in the outer disk is depleted in carbon, with a cor- responding enhancement of carbon-rich ices at the disk midplane. Observations of the carbon content inside of the inner sublimation rim could confirm how much carbon remains locked in kilometer size bodies in the disk.

Aims: I aim to determine the density, temperature, and carbon abundance inside the disk dust sublimation rim in a set of T Tauri stars with full protoplanetary disks.

Methods: Using medium-resolution, near-infrared (0.8 to 2.5 μm) spectra and the new GAIA DR 2 distances, I self-consistently determine the stellar, extinction, veiling, and accretion properties of the 26 stars in my sample. From these values, and non-accreting T Tauri spectral templates, I extract the inner disk excess of the target stars from their observed spectra . Then I identify a series of C0 recombination lines in 18 of these disks and use the CHIANTI atomic line database with an optically thin slab model to constrain the average ne, Te, and nC for these lines in the five disks with a complete set of lines. By comparing these values with other slab models of the inner disk using the Cloudy photoionization code, I also constrain nH and the carbon abundance, XC , and hence the amount of carbon 'missing' from the slab. For one disk, DR Tau, I use relative abundances for the accretion stream from the literature to also determine XS i and XN .

Results: The inner disks modeled here are extremely dense ($n_H \sim 10^{16}$ cm^{-3}), warm ($T_e \sim 4500$ K), and moderately ionized ($\log X_e \sim 3.3$). Three of the five modeled disks show robust carbon depletion up to a factor of 42 relative to the solar value. I discuss multiple ways in which the 'missing' carbon could be locked out of the accreting gas. Given the high-density inner disk gas, evidence for radial drift, and lack of obvious gaps in these three systems, their carbon depletion is most consistent with the 'missing' carbon being sequestered in kilometer size bodies. For DR Tau, nitrogen and silicon are also depleted by factors of 45 and 4, respectively, suggesting that the kilometer size bodies into which the grains are locked were formed beyond the N2 snowline. I explore briefly what improvements in the models and observations are needed to better address this topic in the future.

円盤中の炭素のabundance を近赤外のスペクトルで調べる。

炭素の再結合線から、n_e, T_e, n_C などをスラブモデルを使って得る。

モデルから、円盤内縁はextremely dense(nH~1016 cm-3), warm (Te~4500K),

moderately ionized (log Xe ~3.3)。太陽組成に対して42倍のcarbon depletion -> 微惑星形成で失われた？

35. Measuring the atomic composition of planetary building blocks

Melissa McClure[1], Carsten Dominik[2] and Mihkel Kama[3]

Context: Volatile molecules are critical to terrestrial planetary habitability, yet they are difficult to observe directly where planets form at the midplanes of protoplanetary disks. It is unclear whether the inner ?1 AU of disks are volatile-poor or if this region is resupplied with ice-rich dust from colder disk regions. Dust traps at radial pressure maxima bounding disk gaps can cut off the inner disk from these types of volatile reservoirs. However, the trap retention efficiency and atomic composition of trapped dust have not been measured.
Aims: We present a new technique to measure the absolute atomic abundances in the gas accreting onto T Tauri stars and infer the bulk atomic composition and distribution of midplane solids that have been retained in the disk around the young star TW Hya. Methods. We identify near-infrared atomic line emission from gas-phase material inside the dust sublimation rim of TW Hya. Gaus- sian decomposition of the strongest H Paschen lines isolates the inner disk hydrogen emission. We measure several key elemental abundances, relative to hydrogen, using a chemical photoionization model and infer dust retention in the disk. With a 1D transport model, we determine approximate radial locations and retention efficiencies of dust traps for different elements.
Results: Volatile and refractory elements are depleted from TW Hya's hot gas by factors of ?102 and up to 105, respectively. The abundances of the trapped solids are consistent with a combination of primitive Solar System bodies. Dust traps beyond the CO and N2 snowline cumulatively sequester 96% of the total dust flux, while the trap at 2 AU, near the H2 O snowline, retains 3%. The high depletions of Si, Mg, and Ca are explained by a third trap at 0.3 AU with >95% dust retention.
Conclusion: TW Hya sports a significant volatile reservoir rich in C- and N-ices in its outer submillimeter ring structure. However, unless the inner disk was enhanced in C by earlier radial transport, typical C destruction mechanisms and the lack of a C resupply should leave the terrestrial planet-forming region of TW Hya 'dry' and carbon-poor. Any planets that form within the silicate dust trap at 0.3 AU could resemble Earth in terms of the degree of their volatile depletion.

TW Hya に降着するガスのabundanceや、円盤の含まれる固体成分の組成を調べる。

TW Hyaのhot gas はvolatile やrefractory elements が10^2-10^5 deplete している。

円盤に残った固体成分の組成は太陽組成と無矛盾。など